Stem Cell Research (2015) 14, 211–223

Available online at www.sciencedirect.com

ScienceDirect

www.elsevier.com/locate/scr

The role of microRNA-30c in the self-renewal and differentiation of C6 glioma cells

Chuan-Chuan Chao [a], Daphne Kan [b], Kuo-Shyan Lu [a], Chung-Liang Chien [a,b,*]

[a] Department of Anatomy and Cell Biology, College of Medicine, National Taiwan University, No. 1, Section 1, Jen-Ai Road, Taipei 100, Taiwan
[b] Center of Genomic Medicine, National Taiwan University, 6F., No. 2, Syu-Jhou Road, Taipei 100, Taiwan

Received 22 May 2014; received in revised form 4 January 2015; accepted 26 January 2015
Available online 3 February 2015

Abstract

Background: Sphere formation, one method for identifying self-renewal ability, has been used to report that cancer stem-like cells exist in rat C6 glioma cells. Recent studies suggested that cancer stem-like cells share the stem cell properties of self-renewal and multipotent ability of neural stem cells and might be regulated by microRNAs (miRNAs). However, the mechanism of miRNA involvement in the sphere formation and neural differentiation abilities of cancer stem-like cells is poorly understood. ***Results***: We found that miRNA-30c could assist in sphere formation of C6 cells under defined conditions in neural stem cell medium DMEM/F12-bFGF-EGF-B27. Moreover, overexpression of miRNA-30c might reduce 3-isobutyl-1-methylxanthine (IBMX)-induced neural differentiation, as the expression of neural markers, especially glial fibrillary acidic protein (GFAP), decreased. Further experiments revealed that miRNA-30c inhibited the IBMX-induced astrocyte differentiation via targeting the upstream genes and inactivating phosphorylation of STAT3 of the JAK-STAT3 pathway. Subsequently, the expression of GFAP was reduced and the number of astrocyte differentiation from C6 cells decreased. ***Conclusions***: Our findings suggest that miRNA-30c could play a regulatory role in self-renewal and neural differentiation in C6 glioma cells.

Introduction

A rat C6 glioma cell line was established by repetitively administering *N*, *N*′-nitrosomethylurea to outbred Wistar rats by Benda et al. (1968) and Schmidek et al. (1971). Injecting these C6 cells into newborn rats induced tumors that were consistent with glioblastoma multiforme (GBM) in terms of pathology. Therefore, this C6 glioma cell line can be used for inducing an in vivo experimental astrocytoma model in rats (Auer et al., 1981), investigating the mechanism of tumor growth, angiogenesis, and invasion, and designing anticancer therapies (Abramovitch et al., 1995; Bernstein et al., 1990, 1991; Chicoine and Silbergeld, 1995; Nagano et al., 1993; San-Galli et al., 1989). It also has been proved that C6 cells have the attributes of self-renewal, multipotency, and tumorigenicity, which are the characteristics of cancer stem-like cells (Kondo et al., 2004; Shen et al., 2008; Zheng et al., 2007). In these studies, the ability of self-renewal was characterized by using "sphere formation" under culture conditions including basic fibroblast growth factor (bFGF), epidermal growth factor

* Corresponding author at: No. 1, Section 1, Jen-Ai Road, Taipei 100, Taiwan. Fax: +886 2 23915292.
E-mail address: chien@ntu.edu.tw (C.-L. Chien).

http://dx.doi.org/10.1016/j.scr.2015.01.008
1873-5061/

(EGF), and B27 supplementation. These sphere cells were further confirmed as "cancer stem-like cells" based on their characteristics of multipotency and tumorigenicity.

Some reports suggested that microRNAs (miRNAs) can function as regulators in cancer stem-like cells including GBM tumors, hepatocellular carcinomas, and lung adenocarcinomas (Bushati and Cohen, 2007; Calin and Croce, 2006a,b; Ciafre et al., 2005; Godlewski et al., 2010; Murakami et al., 2006; Yanaihara et al., 2006). MicroRNAs are noncoding sequences that act as "post-transcriptional" regulators that bind to complementary sequences in the 3′-untranslated regions of target mRNA transcripts by imperfect base-pairing, usually resulting in gene silencing (Alvarez-Garcia and Miska, 2005; Bushati and Cohen, 2007). There is some evidence that miRNAs are involved in neural development and tumor formation (Alvarez-Garcia and Miska, 2005; Calin and Croce, 2006b; DeSano and Xu, 2009; Fineberg et al., 2009; Hatfield and Ruohola-Baker, 2008; Kosik, 2006). During neural development, for example, loss of miRNA-9 suppresses proliferation but promotes the migration of human neural progenitor cells in vitro (Delaloy et al., 2010). Zhao et al. reported that miRNA-219 and miRNA-338 were oligodendrocyte-specific miRNAs in the spinal cord of mice, and function in part by directly repressing negative regulators of oligodendrocyte differentiation, including transcription factors Sox6 and Hes5 (Zhao et al., 2010).

Here, we demonstrate that a miRNA microarray served as a good platform for investigating which miRNA contributes in the processes of sphere formation and neural differentiation in this glioma cell model. Spheres were formed at first to enhance the potential for multipotency, and then neural differentiation was induced by 3-isobutyl-1-methylxanthine (IBMX) stimulation. Several miRNAs involved in sphere formation were identified by the miRNA microarray, and miRNA-30c was confirmed to play an important role in sphere formation. Furthermore, miRNA-30c suppressed the expression of glial fibrillary acidic protein (GFAP) by affecting the JAK-STAT3 pathway. These results suggest that miRNA-30c has a regulatory role in self-renewal and neural differentiation.

Material and methods

Cell culture

A rat C6 glioma cell line was purchased from the Bioresource Collection and Research Center (BCRC; Taiwan). Cells were cultured in serum-containing or serum-free neural stem cell medium at a density of 1×10^5 cells/dish. The serum-containing medium was composed of Dubecco's modified Eagle's medium (DMEM) (Life Technologies, Carlsbad, CA, USA), 10% fetal bovine serum (FBS; Life Technologies) and penicillin–streptomycin (Life Technologies). Cells were incubated at 37 °C under 95% air, 5% CO_2, and 100% humidity.

Sphere formation

C6 glioma cells were seeded on 6 cm petri dishes at 1×10^5 cells/dish (Becton Dickinson Labware, Franklin Lakes, NJ, USA). Each dish contained 5 ml serum-free neural stem cell medium DMEM plus F12 containing 20 ng/ml bFGF (Life Technologies), 20 ng/ml EGF (Life Technologies), and 20 μl/ml B27 supplement (Life Technologies) (hitherto designated DMEM/F12-bFGF-EGF-B27). Cells were incubated at 37 °C under 95% air, 5% CO_2, and 100% humidity. Fresh 200 μl lots of serum-free neural stem cell medium were added every 24 h and subculture the cells every 1 week for a minimum of 7 passages. After spheres were formed, cells were subsequently cultured in serum-free neural stem cell medium for further RNA and protein analysis. The samples of adherent cells, spheres at 1st passage and spheres 2nd passage are indicated as C6A, C6S-p1 and C6S-p2, respectively.

Western blot analysis

For preparing protein lysates, cells were washed in cold phosphate-buffered saline (PBS), and then treated with RIPA protein lysis buffer (150 mM NaCl, 1% NP-40, 0.5% deoxycholic acid, 0.1% SDS, 50 mM Tris–HCl at pH 7.5, and 5 mM EDTA) containing a cocktail of protease inhibitors (Roche Applied Science, Mannheim, Germany). The cell debris was removed by centrifugation at 14,000 × *g* for 30 min at 4 °C. The protein concentration in the supernatants compared to standard bovine serum albumin (BSA) concentrations was determined using Bio-Rad protein assay kits (Bio-Rad, Hercules, CA, USA). For each lane of 12% SDS-PAGE gel, 30 μg total proteins of cell lysates was loaded, separated, and subsequently transferred onto PVDF membranes (Bio-Rad). The membranes were probed with specific antibodies against βIII-tubulin (1:500, mouse monoclonal, Sigma-Aldrich, St Louis, MO, USA), 2′, 3′-cyclic nucleotide 3′-phosphodiesterase (CNPase; 1:500, mouse monoclonal; Millipore, Billerica, MA, USA), GFAP (1:500, mouse monoclonal; Sigma-Aldrich), nestin (1;1000, mouse monoclonal; BD Biosciences, San Diego, CA, USA), sox2 (1:1000, rabbit polyclonal; Millipore), p-STAT3 (1;1000, rabbit polyclonal; eBioscience, Inc, San Diego, USA) and STAT3 (1:1000, rabbit polyclonal; eBioscience). An anti-GAPDH antibody (1:25,000, mouse monoclonal; Millipore) was used to probe the GAPDH internal control for equal loading of protein lysates. Immunocomplexes were formed by incubation of the proteins with primary antibodies overnight at 4 °C. Blots were washed and incubated with peroxidase conjugated anti-mouse or anti-rabbit secondary antibodies (GE Healthcare, Milwaukee, WI, USA) for 1 h. Western blot results were detected using an enhanced chemiluminescence western blotting system (Millipore) and film autoradiography (Kodak, Rochester, NY, USA).

Immunofluorescent staining

Cells on poly-D-lysine-coated coverslips (Sigma-Aldrich) were fixed with 4% paraformaldehyde (Sigma-Aldrich) in PBS (pH 7.4) for 10 min. After washing three times with PBS, the cells were then incubated with blocking buffer containing 10% normal goat serum (Life Technologies) and 0.1% Triton X-100 (Sigma-Aldrich) in PBS for 30 min at room temperature. After removing the blocking buffer, samples were incubated overnight with primary antibodies against βIII-tubulin (1:1000, rabbit polyclonal IgG; Sigma-Aldrich), GFAP (1:200, mouse monoclonal; Millipore) or CNPase (1:200, mouse monoclonal IgG; Millipore) at 4 °C. After washing the cells three times with PBS at room temperature, cells were incubated with fluorophore-conjugated secondary antibodies (Sigma-Aldrich) to recognize primary antibodies. Hoechst 33342 (Sigma-Aldrich) was used to label DNA in the cell

nuclei. After washing with PBS three times at room temperature, cells were mounted in fluoromount G (Electron Microscopy Science, EMS, Hatfield, PA, USA). Cells were visualized with a Leica TCS SP5 confocal microscope (Leica Microsystems GmbH, Wetzlar, Germany).

In vitro differentiation

To study neural differentiation, cells were initially seeded at a density of 1×10^5 cells per 6 cm dish in serum-free neural stem cell medium for 7 days to form spheres, then the spheres were dissociated to single cells and plated in serum-free neural stem cell culture medium for another 7 days. For studying the induction of differentiation, serum-free neural stem cell medium was replaced by induction medium, which contained neurobasal medium, 2% FBS, B27 supplement, and IBMX (Sigma-Aldrich) for another 3 days. The stock solution of IBMX was prepared in DMSO (Sigma-Aldrich). During this period, the medium was replaced with fresh induction medium every day.

RNA sample preparation

Total RNA with or without any drug treatment from C6A, C6S-p1 and C6S-p2 was extracted using TRIzol reagent (Life Technologies) and stored at −80 °C. All of the samples underwent a check on the quality and the quantity of sample RNA using an Agilent 2100 Bioanalyzer (Agilent Technologies, Santa Clara, CA, USA) and the RNA 6000 nano kit according to the manufacturer's instructions (Agilent Technologies). Isolated total RNA was further analyzed by miRNA microarray or converted to cDNA for real-time polymerase chain reaction (PCR) analysis.

MicroRNA microarray screening

For this analysis, the febits biochip "Geniom® Biochip microfluidic primer extension assay, MPEA, *Rattus norvegicus*" was used (febit biomed GmbH, Heidelberg, Germany). The probes were designed as the reverse complements of all major mature miRNAs and miRNA star sequences as published in the current Sanger miRBase release (version 14.0 September 2009, http://microrna.sanger.ac.uk/sequences/index.shtml) (Griffiths-Jones et al., 2008) for rats (*R. norvegicus*). Briefly, sample labeling with biotin was carried out by microfluidic-based enzymatic on-chip labeling of miRNAs by MPEA as described (Vorwerk et al., 2008). Following hybridization for 16 h at 42 °C, the biochip was washed automatically and a program for signal enhancement was processed with the Geniom® RT Analyzer (febit biomed GmbH). The resulting images were evaluated using the Geniom Wizard Software. For each array, the median signal intensity was extracted from the raw data file such that for each miRNA intensity, values were calculated corresponding to each replicate copy of miRBase on the array. Following background correction, the intensity values of each miRNA were summarized by their median value. Quantile normalization was applied to normalize the data across different arrays, and all further analyses were carried out using the normalized and background subtracted intensity values. A median value of each miRNA was obtained. To compare the intensities of each miRNA in any pair of samples, qmedian values were calculated as the ratio of median values in the pair. Logqmedian values were calculated as log values of qmedian values. The miRNAs with the C6S/C6A logqmedian values higher than +2 or lower than −2 were listed in Supplemental Table 1.

Expressions of microRNAs in C6 cells

To determine the effects of miRNA oligos on sphere formation ability, cells were cultured in DMEM/F12-bFGF-EGF-B27 medium overnight, then transfected with the 10 pmol of miRNA oligos using the RNAiMAX transfection reagent (Life Technologies) and incubated at 37 °C under 5% CO_2 in air for 1 week. The miRNA oligos include miRNA-30c, anti-miRNA-30c, miR-125bstar, anti-miR-125bstar and nontargeting controls (NC and anti-NC, GenePharma, Shanghai, P. R. China). Sequences of the miRNA oligos are shown in Table 1.

Cell proliferation assay

The WST-1 cell proliferation assay (Roche Applied Science, Mannheim, Germany) was adapted to measure the proliferation of C6 spheres. Cells were seeded at 5000/well in a 96-well plate, and cultured in DMEM/F12-bFGF-EGF-B27 medium with or without miRNA oligos for quantification of cell proliferation. WST-1 reagent was added to each well, incubated at 37 °C for 4 h under 5% CO_2 in air, and then plates were shaken for 1 min. Plates were analyzed optically at 450 nm with a reference wavelength at 600 nm using a microplate multiscan FC ELISA reader (Thermo Fisher Scientific, Waltham, MA, USA).

Construction of miRNA-30c inducible vector and establishment of stable cell lines

The miRNA-30c of double-stranded oligonucleotides was generated for cloning into the lentiviral vector pTRIPz which contained a turbo-red fluorescent protein (turboRFP) sequence as a reporter gene (Open Biosystems; Thermo Fisher Scientific) according to the manufacturer's instructions. All of these constructs were verified by sequence analysis. The empty vector was used as a control.

Subconfluent cells were harvested and resuspended in fresh culture medium at 1×10^7 cells/ml and mixed with 0.5 μg of the constructed plasmids. Then, electroporation was performed using an ECM830 electroporation system (BTX, San Diego, CA, USA) using the LV mode program recommended by the manufacturer as follows: one pulse at 190 V for 70 ms. After electroporation, cells were plated on a 10 cm culture dish and placed at 37 °C under 5% CO_2 in air for 2 weeks. Cells were selected with puromycin (Merck & Co., Inc., Whitehouse Station, NJ, USA) for 14 days. Individual clones were isolated, and cells were incubated in the absence or presence of doxycyclin (dox) and 1 μM pyridone 6 (a jak inhibitor, Millipore) for real-time PCR, Western blot and immunofluorescent staining.

Real-time PCR analysis

For real-time PCR, miRNAs were elongated in a polyadenylation reaction and then reverse transcribed to

Table 1 Sequences of miRNA oligos and primers.

Name	Sequence (5′ to 3′)
Oligos	
MiRNA-30c	UGUAAACAUCCUACACUCUCACUGAGAGUGUAGGAUGUUUACAUU
Anti-miRNA-30c	GCUGAGAGUGUAGGAUGUUUACA
NC	UUCUCCGAACGUGUCACGUTTACGUGACACGUUCGGAGAATT
Anti-NC	CAGUACUUUUGUGUAGUACAA
Primers	
jak1-F	GCCAGTGACACCATCTTGCAAG
jak1-R	ACCCTCTCCCAAGTCACGAATC
socs3-F	GACCAAGAACCTACGCATCCAG
socs3-R	GAAGGTTCCGTCGGTGGTAAAG
pik3cd-F	AGCCTCCTCATCGGCAAAGGTC
pik3cd-R	CCTCACTGCCCTCGAACTTCAC

miRNA first-strand cDNA according to the manufacturer's instructions (Agilent Technologies). Total RNA was reverse transcribed to first-strand cDNA using oligo-dT primers provided in the ThermoScript™ RT-PCR System (Life Technologies). The primers for genes (*jak1*, *socs3*, and *pik3cd*) are shown in Table 1. Real-time PCR was carried out on cDNA using Brilliant II SYBR Green QPCR Master Mix Kits with low Rox (Agilent Technologies) in MX3000P PCR cycler (Agilent Technologies). All reactions were performed in 25 μl volumes using the following PCR program: initial denaturation at 95 °C for 10 min, 40 amplification cycles at 95 °C for 30 s, 60 s at 60 °C, and 60 s at 72 °C. PCR with pure water instead of the template was used as a negative control. Specificity was verified by melting curve analysis and agarose gel electrophoresis. The threshold cycle values of each sample were used in the post-PCR data analysis. GAPDH was used as an internal control for normalization of mRNA levels.

Statistical analysis

The experiments were repeated 3 times and the results of a typical experiment are shown. The experimental data were presented as the mean ± SEM and were evaluated for significance by unpaired Student *t*-test. Statistical significance was established at a level of $p < 0.05$.

Results

Sphere formation and multipotency of C6 cells

To investigate the sphere-forming ability of C6 cells, cells were incubated in serum-free neural stem cell medium containing bFGF, EGF, and B27 supplement for 7 days. Morphological examinations of C6 cells cultured under adherent and sphere culture conditions are shown in Supplementary Fig. 1A. In the adherent culture condition, C6 cells showed fibroblast-like morphology (Supplementary Fig. 1A-1), whereas in sphere culture conditions some of the cells formed spheroids and others attached to the bottom of the dish (Supplementary Fig. 1A-2). Besides, immunoreactivities of sox2 and nestin determine by western blot showed that these two neural stem/progenitor markers expressed in adherent cells and sphere culture till at least passage 7. Protein expression patterns of Sox2, nestin (markers for neural stem cell), βIII-tubulin (a marker of neuron), GFAP (an astrocyte marker), and CNPase (a marker of oligodendrocytes) were examined for differentiation potency of C6 cells in adherent and sphere forms. Using western blot analysis, few immunocomplexes of neural markers were detected in adherent cells, whereas elevated protein levels of βIII-tubulin, GFAP, and CNPase were observed in spheres (Fig. 1A). C6 cells without differentiation induction remained spheroid morphology (Supplementary Fig. 1C-4). Immunoreactivities of GFAP and CNPase, but not βIII-tubulin could be detected by immunocytochemistry of these non-induced C6 sphere cells (Supplementary Figs. 1C-5 and C-6). The results indicated that sphere formation not only promoted the ability of self-renewal (Q. Xu et al., 2009) but also enhanced multipotency.

Differential expression of miRNAs in C6S versus C6A samples

Microarray analysis was performed to identify the miRNAs involved in C6 sphere formation. There are 388 distinct miRNAs included on the array. In C6S cells, 24 miRNAs were obviously upregulated as the C6S/C6A logqmedian values (either C6S-p2/C6A or C6S-p1/C6A) were more than 2 (Supplemental Table 1). 2 miRNAs (miRNA-653 and miRNA-487b) were expressed at much lower levels in the spheres than in the C6 adherent cells. Furthermore, we would like to identify the miRNAs that maintained consistent high levels upon sphere passages. Thus, the miRNAs with C6S-p2/C6S-p1logqmedian values close to zero were selected. Among these miRNAs, miRNA-30c remained high expression levels to at least 7 passages (Fig. 1B) when compared with other chosen miRNAs, such as miR-125bstar. MiRNA-30c has been reported to contribute to developmental processes including osteo differentiation, skeleton formation, adipocyte differentiation, angiogenesis and hepatobiliary (Bridge et al., 2012; Gao et al., 2011; Hand et al., 2009; Karbiener et al., 2011; Vimalraj and Selvamurugan, 2014; Zhang et al., 2012). This study is the first time to report the involvement of miRNA-30c in sphere formation and neural differentiation.

The effects of miRNA-30c oligos in C6 cells

Either miRNA-30c or anti-miRNA-30c oligos were transfected into C6 cells cultured in DMEM/F12-bFGF-EGF-B27 medium.

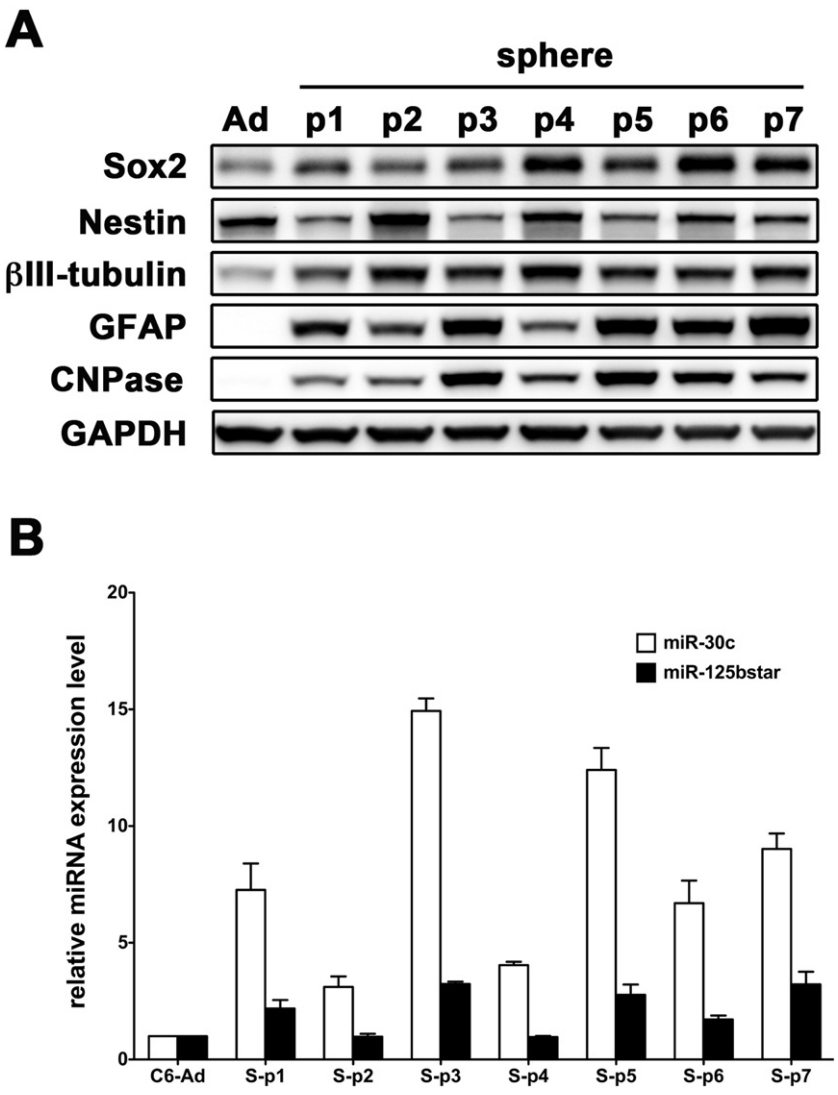

Figure 1 Neural differentiation markers and miRNA expression profiles of adherent and sphere C6 cells during culture passage. (A) Western blot data showed that the expression of βIII-tubulin, GFAP, and CNPase was relatively weak in the adherent cells when compared with the ones in sphere cells, indicating the potential for multipotency in sphere cells. The expression of GAPDH was used as an internal control. (B) Real-time PCR analysis was performed to confirm the increased expression of miRNA-30c in the adherent and sphere C6 cells. The expression of miRNA-125bstar is shown as an example of other selected miRNA from the microarray.

After 7 days, some of the control C6 cells formed spheres and others attached to the bottom of the dishes, showing normal adherent morphology (Fig. 2G). Most C6 cells formed spheres after miRNA-30c treatment (Fig. 2A). The morphology of C6 cells with anti-miRNA-30c treatment was similar to control cells (Fig. 2D). As for the control group, there were no significant effects on sphere formation of C6 cells after NC or anti-NC transfection (Figs. 2C and F). Statistical analysis of the cell proliferation assay results showed that there was no significant difference between the growth rate of the treated and control groups (Fig. 2H).

Overexpression of miRNA-30c in C6 cells

To determine the effects of miRNA-30c on C6 neural differentiation, we constructed a miRNA-30c-inducible plasmid. This construct contained a turbo-red fluorescent protein (turboRFP) sequence as a reporter gene. We then transfected the plasmid into C6 cells and established a stable cell line, named miRNA-30c/C6 cells. The miRNA-30c overexpressing cells formed red spheres when cultured in DMEM/F12-bFGF-EGF-B27 medium. By contrast, the morphology of vector-treated control cells was similar to C6 parental cells and lacked turboRFP protein expression (Supplementary Fig. 2A). Real-time PCR analysis of miRNAs showed an apparent increase of miRNA-30c expression in dox-induced sphere cells (Supplementary Fig. 2B).

MiRNA-30c overexpressing C6 (miR-30c/C6) cells with doxycycline induction were cultured under sphere-forming condition till at least passage 7. The expression of the neural differentiation markers and miRNAs in the cells was characterized by western blot. The results showed that βIII-tubulin, GFAP, and CNPase were expressed less in adherent miR-30c/C6 cells than their average expression levels in sphere cells,

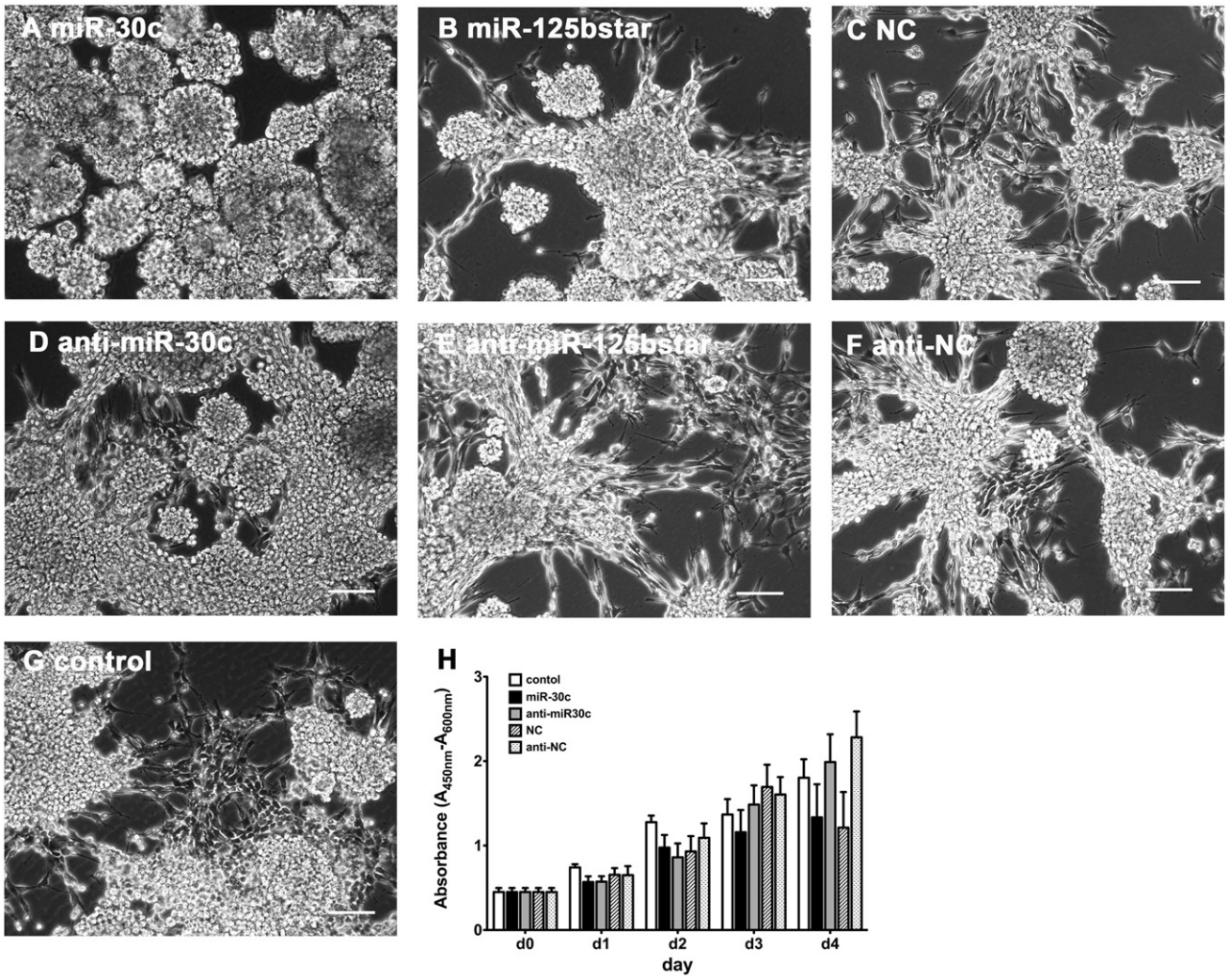

Figure 2 The effects of miRNA oligos on morphology and proliferation ability of C6 cells. C6 cells were cultured in DMEM/F12-bFGF-EGF-B27 medium with (A) miRNA-30c, (B) miR-125bstar, (C) NC (negative control), (D) anti-miRNA-30c, (E) anti-miR-125bstar, (F) anti-NC or (G) without treatments (control) for 7 days. In the control group, in addition to forming spheres, some cells attached to the bottom of dishes and showed normal adherent morphology. Spheres were observed following treatment with miRNA-30c. The morphologies of C6 cells were similar to the control group when treated with anti-miRNA-30c, miR-125bstar, anti-miR-125bstar, NC, and anti-NC. Scale bar = 100 μm. (H) Cell proliferation assay of C6 cells treated with miRNA oligos.

indicating the potential for multipotency in sphere cells. During cell subculture, the expression level of GFAP and CNPase decreased, and increased levels of sox2, nestin and βIII-tubulin were observed with the existence of miRNA-30c overexpression. The expression of turboRFP was the control of miRNA-30c expression. Real-time PCR analysis confirmed that miRNA-30c expressed in the miR-30c/C6 sphere cells (Fig. 3B).

Neural differentiation of C6 cells

Neural differentiation of C6 cells was induced by IBMX, and the expressions of neural markers, including βIII-tubulin, GFAP, and CNPase, were analyzed by western blotting (Supplementary Fig. 2C). We found that these three neural markers were expressed in higher levels in sphere cells compared with adherent cells. The expression levels of these three markers were further increased after IBMX-induced neural differentiation. In sphere cells overexpressing miRNA-30c, the levels of βIII-tubulin and GFAP became lower than in sphere cells with no such overexpression. After IBMX treatment, βIII-tubulin and GFAP expressions in sphere cells were raised. However, the expression levels of these proteins were lower in the dox-induced cells when compared with the cells without dox induction. Furthermore, there was no significant increase in CNPase expression in sphere cells or IBMX-treated cells when compared with the C6A group. Immunofluorescent staining revealed positive results for βIII-tubulin, GFAP, and CNPase in control and miRNA-30c-transfected cells following IBMX treatment, but without dox induction. Thus, IBMX could induce C6 parental cells and miRNA-30c-transfectant cells to differentiate into neuronal cells (Figs. 4A, B), astrocytes (Figs. 4D, E), and oligodendrocytes (Figs. 4G, H) without the need for dox treatment. However, in the IBMX-treated miRNA-30c-overexpressing cells, the numbers

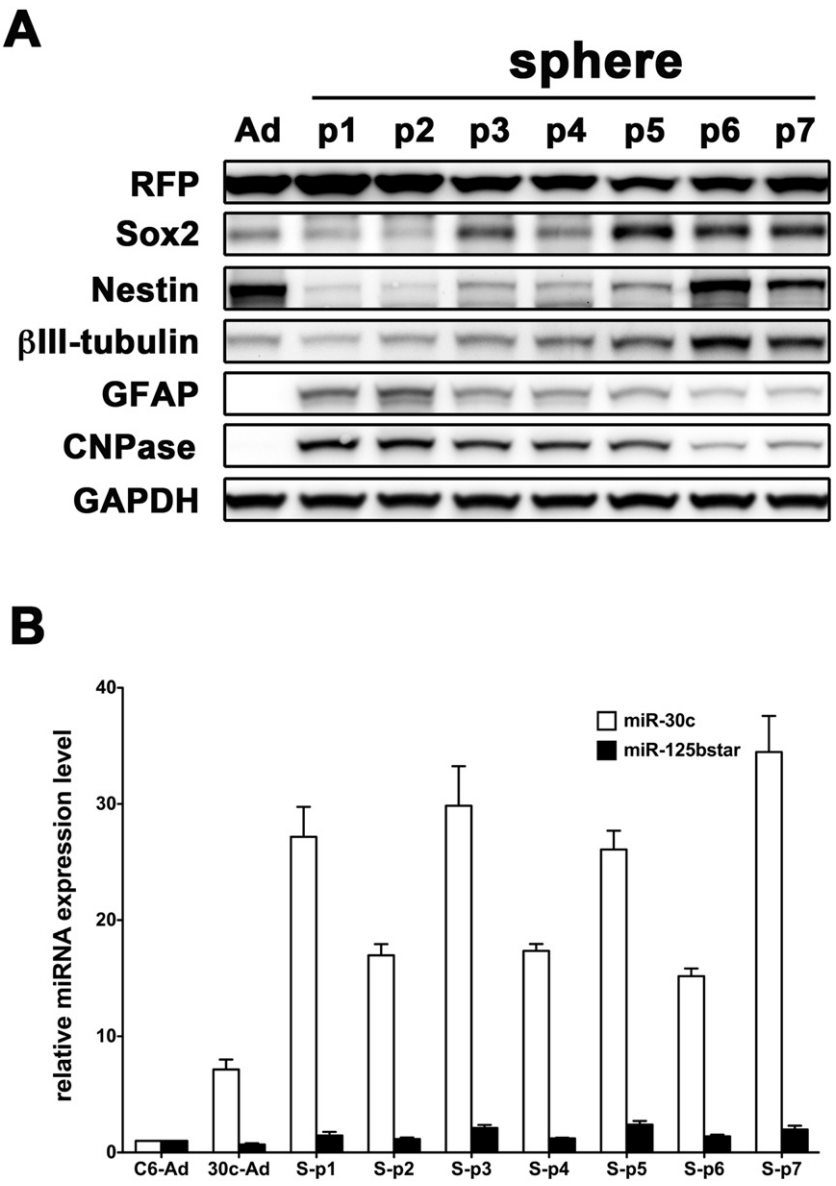

Figure 3 Neural differentiation markers and miRNA expression profiles of miR-30c/C6 cells. (A) Western blot data showed that βIII-tubulin, GFAP, and CNPase were expressed less in adherent miR-30c/C6 cells than the average expression levels in sphere cells, indicating the potential for multipotency in sphere cells. The expression level of GFAP and CNPase decreased, and increased levels of sox2, nestin and βIII-tubulin were observed during subculture. The expression of RFP was the miRNA-30c expression control and GAPDH was used as an internal control. (B) Real-time PCR analysis was performed to examine the expressions of miRNA-30c and miRNA-125bstar in the adherent and sphere cells in C6 adherent cells (C6-Ad), miR-30c/C6 adherent cells (30c-Ad) and miR-30c/C6 sphere cells (S-p1–S-p7).

of βIII-tubulin-positive cells (Fig. 4C) and GFAP-positive cells (Fig. 4F) were reduced, but no significant effect on CNPase-positive cells was seen (Fig. 4I). Thus, miRNA-30c overexpression showed the ability to induce impairment of neural differentiation, especially neurogenesis and astrogenesis. Besides, IBMX can upregulate intracellular cAMP levels thereby possibly activating the protein kinase A (PKA) pathway (Seternes et al., 1999) and accelerate the initiation of differentiation. Thus, IBMX treatment was conducted to test the differentiation ability of C6 cells. The differentiation patterns of C6 sphere cells with and without IBMX-induction were demonstrated by morphology and immunostaining of the molecular markers. After 2-day IBMX treatment on C6 spheres, most cells began to show a neuronal-like morphology, such as bipolar or multipolar processes (Supplementary Fig. 1C-1). GFAP, CNPase, and βIII-tubulin could be detected in some differentiated cells using immunofluorescent staining (Supplementary Figs. 1C-2 and C-3).

Possible pathway

Takanaga et al. reported in 2004 that rising cytoplasmic cAMP could activate the protein kinase A and protein kinase

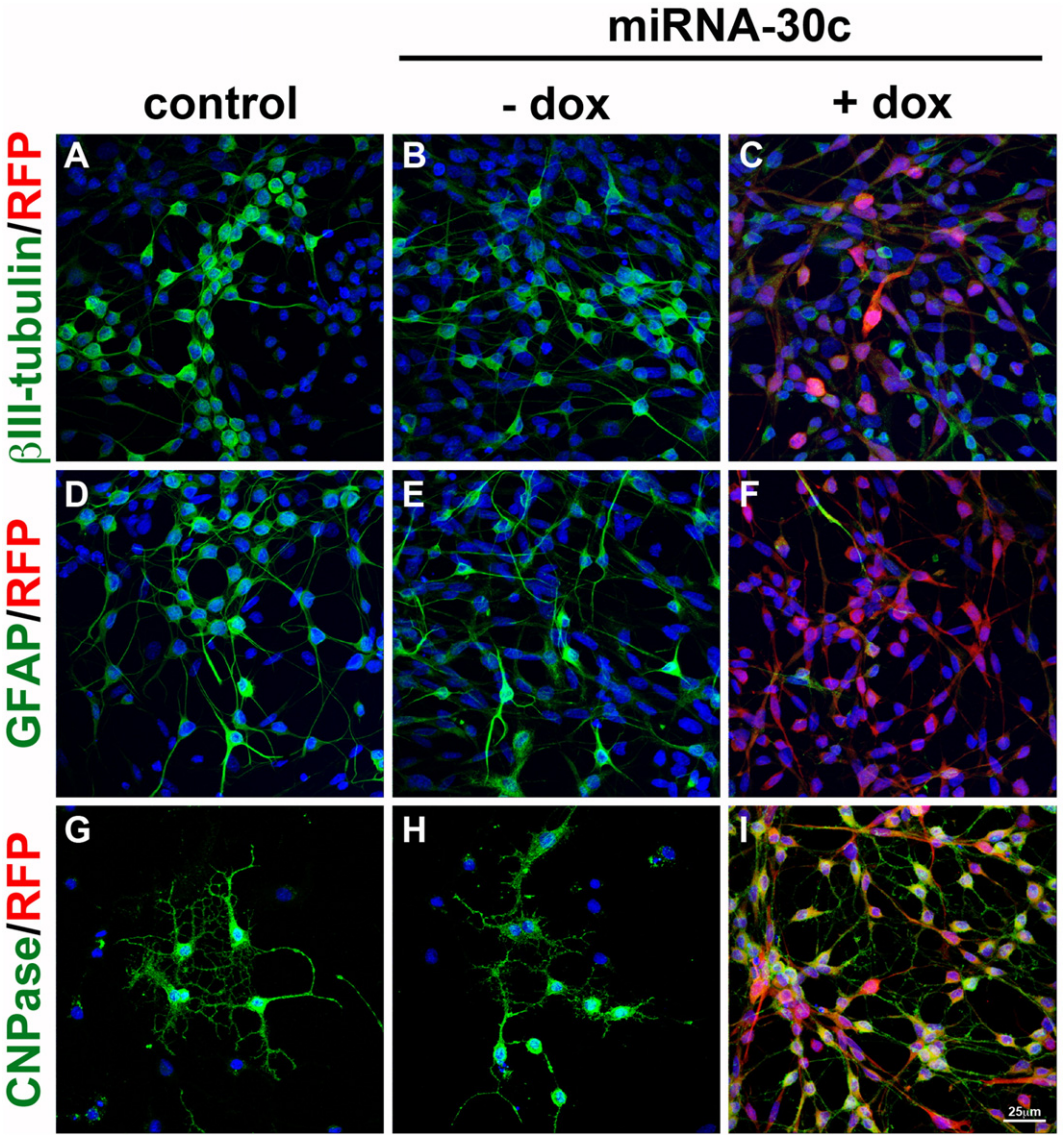

Figure 4 The neural differentiation induced by IBMX in C6 and miRNA-30c/C6 cells demonstrated by immunofluorescence staining. Immunoreactivities for (A–C) βIII-tubulin, (D–F) GFAP, and (G–I) CNPase could be detected after IBMX induction. The expression levels of βIII-tubulin and GFAP were inhibited in dox-treated miRNA-30c/C6 cells (C and F). Scale bar = 25 μm.

C pathways and that the JAK-STAT3 pathway could be activated indirectly (Takanaga et al., 2004). Thus, p-STAT3 expression was increased along with GFAP expression. Our western blotting data confirmed that C6 spheres overexpressed GFAP following IBMX induction (Fig. 6A). However, GFAP expression was inhibited when the cells were treated with miRNA-30c. Therefore, we further examined how miRNA-30c overexpression might affect the expression of p-STAT3 by western blotting analysis. The expression of p-STAT3 was induced in IBMX-induced sphere cells lacking miRNA-30c expression, whereas a lower p-STAT3 protein level was shown when miRNA-30c-overexpressing cells were stimulated with IBMX. The changes of p-STAT3 were similar to the trend of GFAP changes upon IBMX-induced differentiation (Fig. 5). It is possible that some miRNA-30c-related candidate target genes exist in the JAK-STAT3 signaling pathway. The bioinformatics tool RNAhybrid (http://bibiserv.techfak.uni-bielefeld.de/renhybrid/) was employed to identify the JAK-STAT3 pathway-related genes: *pik3cd*, *socs3*, and *jak1*. Real-time PCR analysis of genes in miR-30c/C6 cells showed that in adherent cells, the mRNA levels of *socs3* and *pik3cd* genes in miRNA-30c/C6 cells without dox treatment were lower than in the cells treated with dox. On the contrary, the expression of *jak1* was increased in the miRNA-30c-overexpressing C6 cells. In sphere cells, all these three gene expression levels were decreased in dox-induced miRNA-30c/C6 cells compared with cells lacking dox treatment. Similar to the results for adherent cells, the mRNA expression levels of *pik3cd* and *socs3* were decreased and *jak1* expression was increased in the IBMX-treated, miRNA-30c overexpressing cells. After anti-miRNA-30c oligo treatment, increased expression levels in all these genes compared with the dox-induced miRNA-30c/C6 cells (Figs. 5B–D).

Furthermore, pyridine 6 (a selective Jak1 inhibitor) was used to examine if the inhibition to JAK-STAT pathway might have similar effects with miRNA-30c. Cells were cultured in

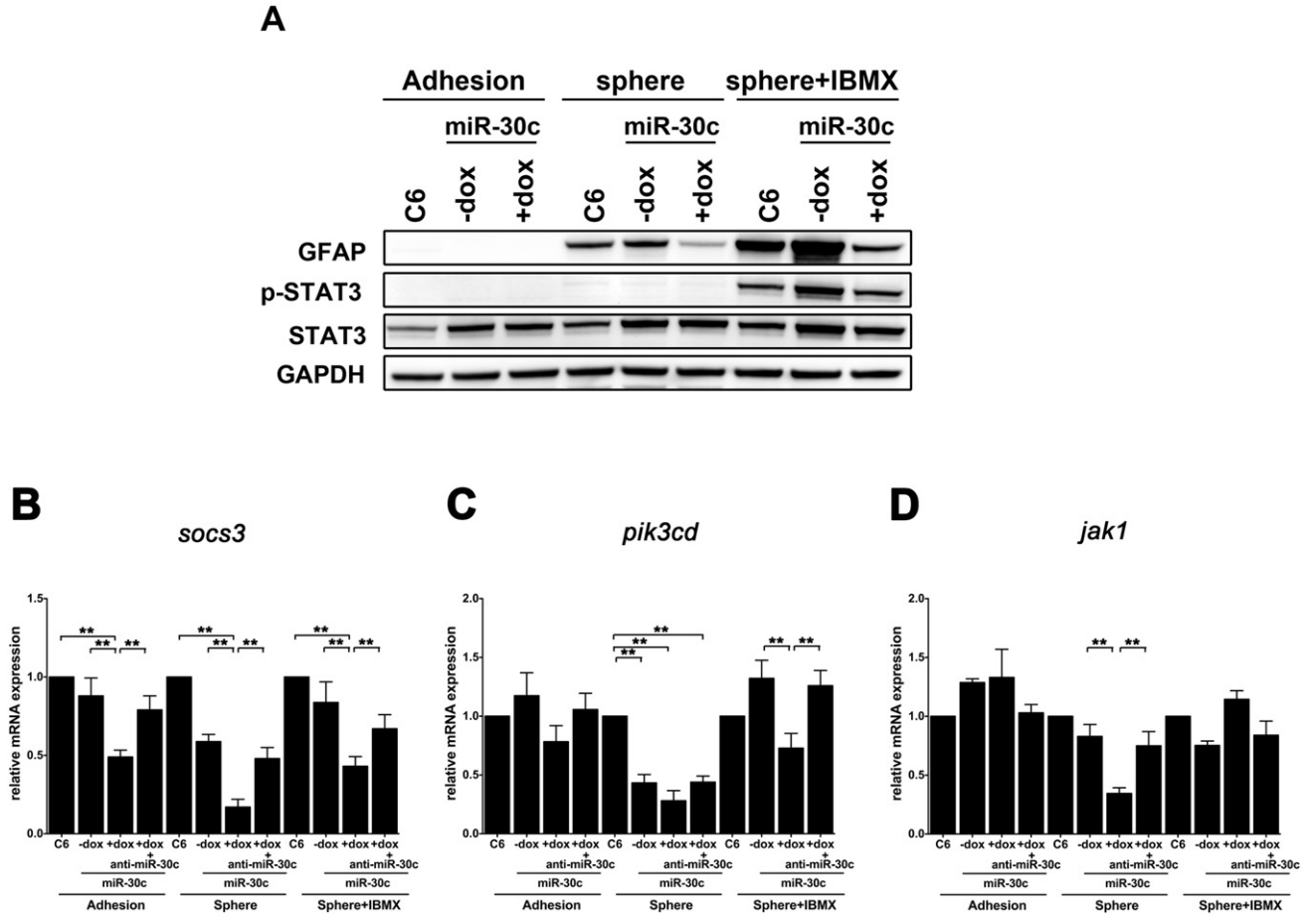

Figure 5 Protein and mRNA expression patterns of p-STAT3 and STAT3 in C6 and miR-30c/C6 cells after IBMX induction. (A) Western blot data showed that the expression of p-STAT3 and total STAT3 could be detected in IBMX-induced cells. Overexpression of miRNA-30c (+dox) suppressed the protein expression of p-STAT3. The expression of GAPDH was an internal control. (B)–(D) Real-time PCR analysis showed that *jak1*, *socs3*, and *pik3cd* were detected in C6 and miR-30c/C6 inducible cells. In adherent cells, overexpression of miRNA-30c reduced the mRNA expression of *socs3* and *pik3cd*, while the mRNA levels of *jak1* was increased. In sphere cells, overexpression of miRNA-30c resulted in decreased expression levels in all these three genes compared with control cells. After IBMX treatment, overexpression of miRNA-30c decreased the mRNA expressions of *socs3* and *pik3cd*, whereas it increased the expression of *jak1*. After being treated with anti-miRNA-30c oligos, increased expression levels in all these genes compared with the dox-induced miRNA-30c/C6 cells (**, $p < 0.01$, unpaired *t*-test, n = 3).

control medium without any treatment, pyridone 6, IBMX or IBMX plus with pyridine 6 for 2 days. Protein lysates were extracted for western blot analysis. The results showed that increasing expression of p-STAT3 could be detected in IBMX-induced cells. Downregulated protein expression levels of GFAP and p-STAT3 in cells after treated with pyridine 6 indicating that astrocyte differentiation were regulated by JAK-STAT3 pathway activation (Fig. 6).

Discussion

Here, we report that rat C6 glioma cells could form spheres in serum-free medium containing bFGF, EGF, and the B27 supplement and differentiate into three different cell lineages: neurons, astrocytes, and oligodendrocytes after IBMX induction. These results are consistent with previous reports suggesting that C6 cells might have the abilities of self-renewal and multipotency (Kondo et al., 2004; Zheng et al., 2007): namely the characteristics of cancer stem-like cells. In serum-free medium containing bFGF and EGF, sphere formation is a simple and effective method for the isolation and enrichment of cancer stem-like cells in human and murine cell lines as well as rat C6 cells (Pellegatta et al., 2006; Yu et al., 2008). The increased expression of neural markers in both sphere cells and IBMX-induced sphere cells indicated that the ability for neural differentiation could be induced in sphere-forming cells. These results were consistent with the studies of Kondo et al. (2004) and Yu et al. (2008). In summary, sphere-forming cells can be enriched in C6 cells and can differentiate into neural cells including neurons, astrocytes, and oligodendrocytes.

A miRNA microarray was applied for investigating the effects of miRNAs in sphere formation in C6 cells. Supplemental Table 1

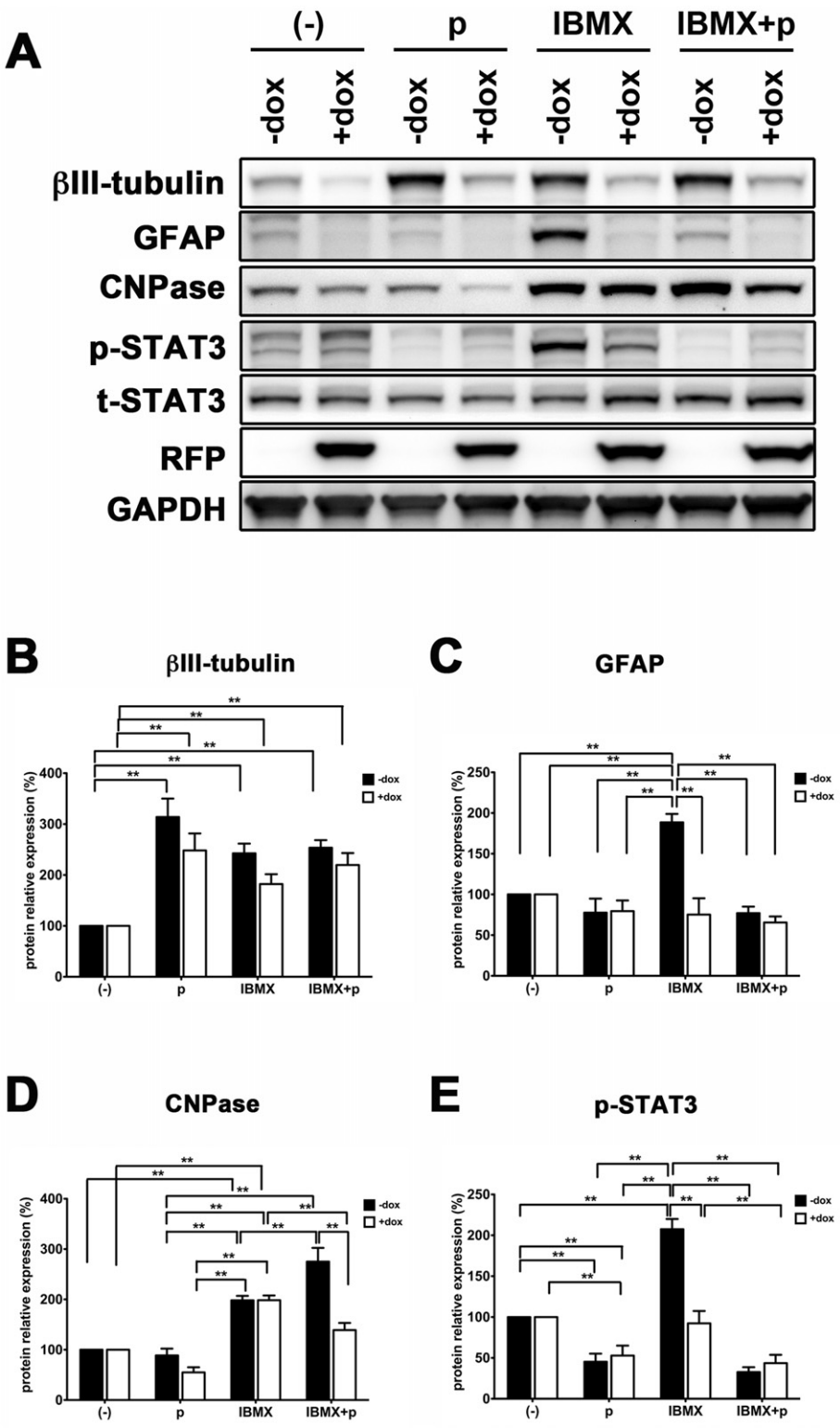

Figure 6 Decreasing of GFAP expression by through blocking of Jak-STAT3 pathway. MiR-30c/C6 cells were cultured in control medium without any treatment ((−)), pyridone 6 (p, a selective Jak1 inhibitor), IBMX or IBMX plus with pyridine 6 (IBMX + p) for 2 days. Protein lysates were extracted for western blot analysis (A). The results showed that increasing expression of p-STAT3 could be detected in IBMX-induced cells. Downregulated protein expression levels of GFAP and p-STAT3 in cells after being treated with pyridone 6 indicating that astrocyte differentiation were regulated by JAK-STAT3 pathway activation. The expression of GAPDH was an internal control. (B–E) Relative signal intensities for βIII-tubulin (B), GFAP (C), CNPase (D) and p-STAT3 (E) in the western blot analysis. Increased expression of βIII-tubulin, GFAP, CNPase and p-STAT3 were shown in control and miRNA-30c-overexpressed cells after IBMX stimulation except GFAP expression in miRNA-30c-induced cells. Only expression of GFAP and p-STAT3 were impeded when IBMX-treated cells were incubated under the existence of pyridone 6 (**, $p < 0.01$, unpaired *t*-test, n = 3).

shows that 24 miRNAs were upregulated and two were downregulated in sphere-forming cells compared with adherent cells. Most of these miRNAs play a suppressive role in carcinogenesis. MicroRNA-9 is highly expressed in glioma cells, and inhibits cell proliferation by targeting CREB, a target of miRNA-9, suggesting the possibility of a "miRNA-9–CREB" minicircuitry involved in coordinating the proliferation of glioma cells (Tan et al., 2012). MicroRNA-146a inhibits cell growth, cell migration, and induces apoptosis in non-small-cell lung cancer cells (Chen et al., 2013). It acts as a native safeguarding mechanism to restrict the formation of glioma stem-like cells and glioma growth by directly controlling the expression of Notch1 (Mei et al., 2011). MicroRNA-34a acts as a putative tumor suppressor by inhibiting cell proliferation through mediating gene expression of notch1 in GBM (Li et al., 2011). In glioma cells, overexpressed miRNA-26a might play a vital role in promoting tumor growth and angiogenesis by suppressing PHB and the downstream AKT and ERK pathways (Qian et al., 2013). By targeting OCT4, miRNA-145 suppresses lung adenocarcinoma-initiating cell proliferation (Yin et al., 2011). Furthermore, some of these miRNAs are associated with cell differentiation. For example, miRNA-9 plays a regulatory role that coordinates the proliferation and migration of human neural progenitor cells (Delaloy et al., 2010). In addition, miRNA-9 might be involved in neural stem cell self-renewal and differentiation by suppressing TLX expression, inhibiting neural stem cell proliferation, and accelerating neural differentiation (Zhao et al., 2009). Overexpression of miRNA-204 inhibited osteoblast differentiation and promoted adipocyte differentiation by directly targeting Runx2 in mesenchymal progenitor cells and bone marrow stromal cells (Huang et al., 2010). MicroRNA-199a-5p and miRNA-145 were shown to be involved in oligodendrocyte development by mediating *C11Orf9* repression (Letzen et al., 2010). MicroRNA-145 has also been reported to play an important role in human stem cell growth and differentiation by regulating OCT4, SOX2, and KLF4 (N. Xu et al., 2009). During neuronal development, miRNA-34a plays a role in hippocampal spinal morphology and electrophysiological change through the Tap73/miRNA-34a axis in mouse embryonic stem cells (Agostini et al., 2011). In this study, we found that these miRNAs were upregulated when cells formed spheres in DMEM/F12-bFGF-EGF-B27 medium, indicating that these miRNAs might play regulatory roles in cancer progression and differentiation.

It is the first time to report the involvement of miRNA-30c in enhancing sphere formation and neural differentiation. The relationships of miRNA-30c and osteodifferentiation and adipocyte differentiation have been discussed previously (Gao et al., 2011; Karbiener et al., 2011; Vimalraj and Selvamurugan, 2014). We will further analyze if miR-30c-overexpression affects the expression of miR124a or miR9 (miRNAs known to play a key role in neurogenesis) and miRNA-199a-5p and miRNA-145 (oligodendrocyte development). The protein expression level of GFAP was inhibited in miRNA-30c-overexpressing sphere cells after IBMX induction compared with the control group. By elevating the level of intracellular cAMP, IBMX is known to induce the astrocytic differentiation of C6 glioma cells by activating the JAK-STAT pathway (Bonni et al., 1997; Takanaga et al., 2004). In the present experiments, the protein level of p-STAT3 was also decreased in miRNA-30c-overexpressing IBMX-induced C6 sphere cells. In Moorthi's report, the JAK-STAT3 pathway was affected by miRNA-30c, suggesting that target genes might exist in this pathway (Moorthi et al., 2013). Here, *pik3cd*, *socs3*, and *jak1*, the putative target genes for miRNA-30c in the JAK-STAT3 pathway, were examined by real-time PCR. The decreased mRNA levels of *pik3cd* and *socs3* might explain the inhibited p-STAT3 expression in miRNA-30c-overexpressing IBMX-induced C6 cells (Fig. 7). Qin et al. reported that the activation of STAT3 leads to SOCS3 expression in astrocyte cultures (Qin et al., 2008). In Baker's study, oncostatin M stimulated cultured astrocytes and induced SOCS3 expression; the expression decreased with time and p-STAT3 showed similar expression pattern as SOCS3 (Baker et al., 2008). When SOCS3 was expressed in neural stem cells, the number of MAP2-positive cells increased and the number of GFAP-positive cells decreased, indicating that overexpression of SOCS3 can regulate neurogenesis and astrogenesis in neural stem cells (Cao et al., 2006). These results might help us to identify the miRNA-30c-regulated target genes acting during neural differentiation.

Conclusions

In summary, we have provided evidence that miRNA-30c plays an important role in sphere formation and neural differentiation in glioma cells. Although the interactions between miRNA-30c and its related genes are not yet clear, this study might offer a new way to examine the regulatory role of miRNAs in the progression of gliomas.

List of abbreviations

bFGF	basic fibroblast growth factor
CNPase	2′,3′-cyclic nucleotide 3′-phosphodiesterase
DMEM	Dulbecco's modified Eagle's medium
Dox	doxycycline
EGF	epidermal growth factor
GBM	glioblastoma multiforme
GFAP	glial fibrillary acidic protein
IBMX	3-isobutyl-1-methylxanthine
miRNA	microRNA
PKA	protein kinase A
turboRFP	turbo-red fluorescent protein

Authors' contributions

CCC carried out all experiments in the study and helped to draft the manuscript with DK. CLC and KSL conceived of the study and participated in its design and coordination as well as revised the manuscript. All authors read and approved the final manuscript.

Acknowledgments

This work was supported by grants to C.-L. Chien (MOST102-2321-B-002-032 and NSC-98-3111-B-002-004) from the Ministry of Science and Technology, Taiwan. The facilities provided by grants from the Ministry of Education, Taiwan to the Center of Genomic Medicine in National Taiwan University are also acknowledged.

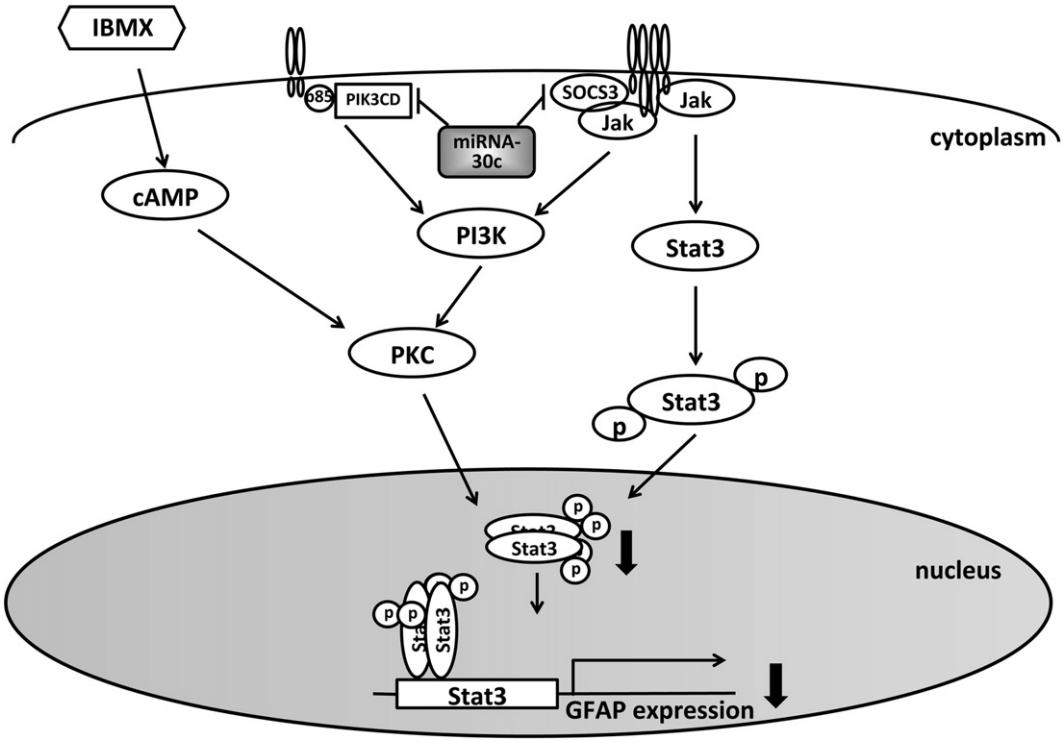

Figure 7 The possible mechanism by which miRNA-30c regulates GFAP expression. Following IBMX stimulation, increased intracellular cAMP level results in upregulation of p-STAT3 and GFAP expression. Treatment with miRNA-30c inhibits the expression of upstream genes of the JAK-STAT3 pathway including *socs3* and *pik3cd*. This then decreases GFAP expression by inhibiting the expression level of p-STAT3.

Appendix A. Supplementary data

Supplementary data to this article can be found online at http://dx.doi.org/10.1016/j.scr.2015.01.008.

References

Abramovitch, R., Meir, G., Neeman, M., 1995. Neovascularization induced growth of implanted C6 glioma multicellular spheroids: magnetic resonance microimaging. Cancer Res. 55, 1956–1962.

Agostini, M., Tucci, P., Steinert, J.R., Shalom-Feuerstein, R., Rouleau, M., Aberdam, D., Forsythe, I.D., Young, K.W., Ventura, A., Concepcion, C.P., Han, Y.C., Candi, E., Knight, R.A., Mak, T.W., Melino, G., 2011. MicroRNA-34a regulates neurite outgrowth, spinal morphology, and function. Proc. Natl. Acad. Sci. U. S. A. 108, 21099–21104.

Alvarez-Garcia, I., Miska, E.A., 2005. MicroRNA functions in animal development and human disease. Development 132, 4653–4662.

Auer, R.N., Del Maestro, R.F., Anderson, R., 1981. A simple and reproducible experimental in vivo glioma model. Can. J. Neurol. Sci. 8, 325–331.

Baker, B.J., Qin, H., Benveniste, E.N., 2008. Molecular basis of oncostatin M-induced SOCS-3 expression in astrocytes. Glia 56, 1250–1262.

Benda, P., Lightbody, J., Sato, G., Levine, L., Sweet, W., 1968. Differentiated rat glial cell strain in tissue culture. Science 161, 370–371.

Bernstein, J.J., Goldberg, W.J., Laws Jr., E.R., Conger, D., Morreale, V., Wood, L.R., 1990. C6 glioma cell invasion and migration of rat brain after neural homografting: ultrastructure. Neurosurgery 26, 622–628.

Bernstein, J.J., Laws Jr., E.R., Levine, K.V., Wood, L.R., Tadvalkar, G., Goldberg, W.J., 1991. C6 glioma-astrocytoma cell and fetal astrocyte migration into artificial basement membrane: a permissive substrate for neural tumors but not fetal astrocytes. Neurosurgery 28, 652–658.

Bonni, A., Sun, Y., Nadal-Vicens, M., Bhatt, A., Frank, D.A., Rozovsky, I., Stahl, N., Yancopoulos, G.D., Greenberg, M.E., 1997. Regulation of gliogenesis in the central nervous system by the JAK-STAT signaling pathway. Science 278, 477–483.

Bridge, G., Monteiro, R., Henderson, S., Emuss, V., Lagos, D., Georgopoulou, D., Patient, R., Boshoff, C., 2012. The microRNA-30 family targets DLL4 to modulate endothelial cell behavior during angiogenesis. Blood 120, 5063–5072.

Bushati, N., Cohen, S.M., 2007. microRNA functions. Annu. Rev. Cell Dev. Biol. 23, 175–205.

Calin, G.A., Croce, C.M., 2006a. MicroRNA-cancer connection: the beginning of a new tale. Cancer Res. 66, 7390–7394.

Calin, G.A., Croce, C.M., 2006b. MicroRNA signatures in human cancers. Nat. Rev. Cancer 6, 857–866.

Cao, F., Hata, R., Zhu, P., Ma, Y.J., Tanaka, J., Hanakawa, Y., Hashimoto, K., Niinobe, M., Yoshikawa, K., Sakanaka, M., 2006. Overexpression of SOCS3 inhibits astrogliogenesis and promotes maintenance of neural stem cells. J. Neurochem. 98, 459–470.

Chen, G., Umelo, I.A., Lv, S., Teugels, E., Fostier, K., Kronenberger, P., Dewaele, A., Sadones, J., Geers, C., De Greve, J., 2013. miR-146a inhibits cell growth, cell migration and induces apoptosis in non-small cell lung cancer cells. PLoS One 8, e60317.

Chicoine, M.R., Silbergeld, D.L., 1995. Invading C6 glioma cells maintaining tumorigenicity. J. Neurosurg. 83, 665–671.

Ciafre, S.A., Galardi, S., Mangiola, A., Ferracin, M., Liu, C.G., Sabatino, G., Negrini, M., Maira, G., Croce, C.M., Farace, M.G.,

2005. Extensive modulation of a set of microRNAs in primary glioblastoma. Biochem. Biophys. Res. Commun. 334, 1351–1358.
Delaloy, C., Liu, L., Lee, J.A., Su, H., Shen, F., Yang, G.Y., Young, W.L., Ivey, K.N., Gao, F.B., 2010. MicroRNA-9 coordinates proliferation and migration of human embryonic stem cell-derived neural progenitors. Cell Stem Cell 6, 323–335.
DeSano, J.T., Xu, L., 2009. MicroRNA regulation of cancer stem cells and therapeutic implications. AAPS J. 11, 682–692.
Fineberg, S.K., Kosik, K.S., Davidson, B.L., 2009. MicroRNAs potentiate neural development. Neuron 64, 303–309.
Gao, J., Yang, T., Han, J., Yan, K., Qiu, X., Zhou, Y., Fan, Q., Ma, B., 2011. MicroRNA expression during osteogenic differentiation of human multipotent mesenchymal stromal cells from bone marrow. J. Cell. Biochem. 112, 1844–1856.
Godlewski, J., Newton, H.B., Chiocca, E.A., Lawler, S.E., 2010. MicroRNAs and glioblastoma; the stem cell connection. Cell Death Differ. 17, 221–228.
Griffiths-Jones, S., Saini, H.K., van Dongen, S., Enright, A.J., 2008. miRBase: tools for microRNA genomics. Nucleic Acids Res. 36, D154–D158.
Hand, N.J., Master, Z.R., Eauclaire, S.F., Weinblatt, D.E., Matthews, R.P., Friedman, J.R., 2009. The microRNA-30 family is required for vertebrate hepatobiliary development. Gastroenterology 136, 1081–1090.
Hatfield, S., Ruohola-Baker, H., 2008. microRNA and stem cell function. Cell Tissue Res. 331, 57–66.
Huang, J., Zhao, L., Xing, L., Chen, D., 2010. MicroRNA-204 regulates Runx2 protein expression and mesenchymal progenitor cell differentiation. Stem Cells 28, 357–364.
Karbiener, M., Neuhold, C., Opriessnig, P., Prokesch, A., Bogner-Strauss, J.G., Scheideler, M., 2011. MicroRNA-30c promotes human adipocyte differentiation and co-represses PAI-1 and ALK2. RNA Biol. 8, 850–860.
Kondo, T., Setoguchi, T., Taga, T., 2004. Persistence of a small subpopulation of cancer stem-like cells in the C6 glioma cell line. Proc. Natl. Acad. Sci. U. S. A. 101, 781–786.
Kosik, K.S., 2006. The neuronal microRNA system. Nat. Rev. Neurosci. 7, 911–920.
Letzen, B.S., Liu, C., Thakor, N.V., Gearhart, J.D., All, A.H., Kerr, C.L., 2010. MicroRNA expression profiling of oligodendrocyte differentiation from human embryonic stem cells. PLoS One 5, e10480.
Li, W.B., Ma, M.W., Dong, L.J., Wang, F., Chen, L.X., Li, X.R., 2011. MicroRNA-34a targets notch1 and inhibits cell proliferation in glioblastoma multiforme. Cancer Biol. Ther. 12, 477–483.
Mei, J., Bachoo, R., Zhang, C.L., 2011. MicroRNA-146a inhibits glioma development by targeting Notch1. Mol. Cell. Biol. 31, 3584–3592.
Moorthi, A., Vimalraj, S., Avani, C., He, Z., Partridge, N.C., Selvamurugan, N., 2013. Expression of microRNA-30c and its target genes in human osteoblastic cells by nano-bioglass ceramic-treatment. Int. J. Biol. Macromol. 56, 181–185.
Murakami, Y., Yasuda, T., Saigo, K., Urashima, T., Toyoda, H., Okanoue, T., Shimotohno, K., 2006. Comprehensive analysis of microRNA expression patterns in hepatocellular carcinoma and non-tumorous tissues. Oncogene 25, 2537–2545.
Nagano, N., Sasaki, H., Aoyagi, M., Hirakawa, K., 1993. Invasion of experimental rat brain tumor: early morphological changes following microinjection of C6 glioma cells. Acta Neuropathol. 86, 117–125.
Pellegatta, S., Poliani, P.L., Corno, D., Menghi, F., Ghielmetti, F., Suarez-Merino, B., Caldera, V., Nava, S., Ravanini, M., Facchetti, F., Bruzzone, M.G., Finocchiaro, G., 2006. Neurospheres enriched in cancer stem-like cells are highly effective in eliciting a dendritic cell-mediated immune response against malignant gliomas. Cancer Res. 66, 10247–10252.
Qian, X., Zhao, P., Li, W., Shi, Z.M., Wang, L., Xu, Q., Wang, M., Liu, N., Liu, L.Z., Jiang, B.H., 2013. MicroRNA-26a promotes tumor growth and angiogenesis in glioma by directly targeting prohibitin. CNS Neurosci. Ther 9, 804–812.
Qin, H., Niyongere, S.A., Lee, S.J., Baker, B.J., Benveniste, E.N., 2008. Expression and functional significance of SOCS-1 and SOCS-3 in astrocytes. J. Immunol. 181, 3167–3176.
San-Galli, F., Vrignaud, P., Robert, J., Coindre, J.M., Cohadon, F., 1989. Assessment of the experimental model of transplanted C6 glioblastoma in Wistar rats. J. Neurooncol. 7, 299–304.
Schmidek, H.H., Nielsen, S.L., Schiller, A.L., Messer, J., 1971. Morphological studies of rat brain tumors induced by N-nitrosomethylurea. J. Neurosurg. 34, 335–340.
Seternes, O.M., Sorensen, R., Johansen, B., Moens, U., 1999. Activation of protein kinase A by dibutyryl cAMP treatment of NIH 3T3 cells inhibits proliferation but fails to induce Ser-133 phosphorylation and transcriptional activation of CREB. Cell. Signal. 11, 211–219.
Shen, G., Shen, F., Shi, Z., Liu, W., Hu, W., Zheng, X., Wen, L., Yang, X., 2008. Identification of cancer stem-like cells in the C6 glioma cell line and the limitation of current identification methods. In Vitro Cell. Dev. Biol. Anim. 44, 280–289.
Takanaga, H., Yoshitake, T., Hara, S., Yamasaki, C., Kunimoto, M., 2004. cAMP-induced astrocytic differentiation of C6 glioma cells is mediated by autocrine interleukin-6. J. Biol. Chem. 279, 15441–15447.
Tan, X., Wang, S., Yang, B., Zhu, L., Yin, B., Chao, T., Zhao, J., Yuan, J., Qiang, B., Peng, X., 2012. The CREB-miR-9 negative feedback minicircuitry coordinates the migration and proliferation of glioma cells. PLoS One 7, e49570.
Vimalraj, S., Selvamurugan, N., 2014. MicroRNAs expression and their regulatory networks during mesenchymal stem cells differentiation toward osteoblasts. Int. J. Biol. Macromol. 66, 194–202.
Vorwerk, S., Ganter, K., Cheng, Y., Hoheisel, J., Stahler, P.F., Beier, M., 2008. Microfluidic-based enzymatic on-chip labeling of miRNAs. Nat. Biotechnol. 25, 142–149.
Xu, N., Papagiannakopoulos, T., Pan, G., Thomson, J.A., Kosik, K.S., 2009a. MicroRNA-145 regulates OCT4, SOX2, and KLF4 and represses pluripotency in human embryonic stem cells. Cell 137, 647–658.
Xu, Q., Yuan, X., Tunici, P., Liu, G., Fan, X., Xu, M., Hu, J., Hwang, J.Y., Farkas, D.L., Black, K.L., Yu, J.S., 2009b. Isolation of tumour stem-like cells from benign tumours. Br. J. Cancer 101, 303–311.
Yanaihara, N., Caplen, N., Bowman, E., Seike, M., Kumamoto, K., Yi, M., Stephens, R.M., Okamoto, A., Yokota, J., Tanaka, T., Calin, G.A., Liu, C.G., Croce, C.M., Harris, C.C., 2006. Unique microRNA molecular profiles in lung cancer diagnosis and prognosis. Cancer Cell 9, 189–198.
Yin, R., Zhang, S., Wu, Y., Fan, X., Jiang, F., Zhang, Z., Feng, D., Guo, X., Xu, L., 2011. MicroRNA-145 suppresses lung adenocarcinoma-initiating cell proliferation by targeting OCT4. Oncol. Rep. 25, 1747–1754.
Yu, S.C., Ping, Y.F., Yi, L., Zhou, Z.H., Chen, J.H., Yao, X.H., Gao, L., Wang, J.M., Bian, X.W., 2008. Isolation and characterization of cancer stem cells from a human glioblastoma cell line U87. Cancer Lett. 265, 124–134.
Zhang, Y., Xie, R.L., Gordon, J., LeBlanc, K., Stein, J.L., Lian, J.B., van Wijnen, A.J., Stein, G.S., 2012. Control of mesenchymal lineage progression by microRNAs targeting skeletal gene regulators Trps1 and Runx2. J. Biol. Chem. 287, 21926–21935.
Zhao, C., Sun, G., Li, S., Shi, Y., 2009. A feedback regulatory loop involving microRNA-9 and nuclear receptor TLX in neural stem cell fate determination. Nat. Struct. Mol. Biol. 16, 365–371.
Zhao, X., He, X., Han, X., Yu, Y., Ye, F., Chen, Y., Hoang, T., Xu, X., Mi, Q.S., Xin, M., Wang, F., Appel, B., Lu, Q.R., 2010. MicroRNA-mediated control of oligodendrocyte differentiation. Neuron 65, 612–626.
Zheng, X., Shen, G., Yang, X., Liu, W., 2007. Most C6 cells are cancer stem cells: evidence from clonal and population analyses. Cancer Res. 67, 3691–3697.